DETECTION AND FOCUSED IMAGING OF MOVING OBJECTS EVALUATING A SEQUENCE OF SINGLE–LOOK SAR IMAGES *

Martin Kirscht
Institut für Theoretische Nachrichtentechnik und Informationsverarbeitung, Universität Hannover
Appelstr. 9A, D–30167 Hannover, Germany
Phone: +49 511 762–5305, Fax: +49 511 762–5333, Email: kirscht@tnt.uni–hannover.de

ABSTRACT

In multilook synthetic aperture radar (SAR) images moving objects appear defocused when their azimuth velocity component is non–zero. Therefore, they are difficult to detect in such images unless the azimuth velocity component has been compensated. Here, a method for detection of arbitrarily moving ground–based objects and for estimation and compensation of the azimuth velocity component is presented, which is based on evaluation of the temporal correlation in a sequence of single–look SAR images. These images are processed using different look center frequencies and therefore show the ground at different look angles and at different times. Thus, the velocities of the objects can be estimated by tracking the moving objects from image to image. Afterwards, the azimuth velocity component of the objects is compensated. By superimposing the compensated single–look images, a high quality multilook image with focused moving objects is obtained. The achieved absolute relative error of the azimuth velocity component is less than 11 %.

1.0 INTRODUCTION

Synthetic aperture radar (SAR) is an active, all weather capable system to produce high resolution images of the ground. In order to get a high resolution in azimuth (along–track) direction a synthetic aperture is formed during the observation interval, exploiting the relative motion between the platform and the ground. This results in image errors when objects on the ground move themselves. Depending on the direction of the motion two main errors occur. An object which moves in azimuth direction or is accelerated in range direction appears defocused in azimuth direction whereas a range moving object is shifted in azimuth direction in the SAR image (Raney, 1971). In order to compensate these errors it is necessary to detect the moving objects and to estimate their velocities.

For detection of moving objects and for moving target imaging (MTI) some algorithms have been proposed. They usually work on range compressed SAR raw data, either transformed to the Doppler frequency domain (e. g. Freeman, 1987, D'Addio, 1994), or to a time–frequency domain (Barbarossa, 1994). Freeman and Currie proposed a division of the Doppler spectrum into four bands, where one band contains the clutter and the other ones the range moving targets. Either a conventional SAR image or images of the moving targets can be generated. Chen and McGillem additionally compensate the range velocity component by shifting the spectra of the targets towards the clutter spectrum. In the SAR image the range moving objects appear at the right positions provided the antenna beamwidth is small (Chen, 1992).

* Presented at the Third International Airborne Remote Sensing Conference and Exhibition, 7–10 July 1997, Copenhagen, Denmark.

A restriction of these algorithms is that the pulse repetition frequency (PRF) has to be at least four times higher than the Doppler bandwidth of the clutter. To fulfill this condition, either the clutter bandwidth and concurrently the resolution in azimuth direction has to be reduced as done in (Chen, 1992), or the PRF has to be increased with the disadvantage of a more complex SAR system. However, the detection of objects with an azimuth velocity component only is not possible by applying these algorithms.

In this paper, a new method for detection of arbitrarily moving ground–based objects and for the estimation and compensation of the azimuth velocity component is presented. This method works with a PRF which is only a little higher than the clutter bandwidth and is based on the evaluation of the temporal correlation in a sequence of single–look SAR images. These images are processed from different frequency bands taken out of the Doppler spectrum, i. e. they have different look center frequencies. This implies that the images show the ground at different look angles and therefore at different times. Thus, in each image the moving objects appear at different positions and therefore can be detected. The velocities of the objects are obtained by estimating their displacements in successive images using a block matching algorithm. Afterwards, the moving objects are shifted to a reference position in order to compensate the azimuth velocity component. By superimposing the compensated single–look images, a high quality multilook image with focused moving objects on the background is obtained.

The following chapters of the paper describe the generation of the sequence of single–look SAR images, the detection and velocity estimation algorithm, and the compensation of the azimuth velocity component in order to get a focused image with the moving objects. The paper finishes with experimental results and a conclusion.

2.0 GENERATION OF THE SEQUENCE OF SINGLE–LOOK SAR IMAGES

The generation of the sequence of single–look SAR images is carried out as follows. First, the Doppler spectrum of the range compressed SAR raw data is calculated by performing a fast Fourier transform (FFT) in azimuth direction. Then the Doppler spectrum is subdivided into several overlapping bands and a single–look image is processed from each band. The images show the ground at different (horizontal) look angles θ_i, which depend on the look center frequencies f_{li}, as given by

$$\theta_i = -\arcsin\frac{f_{li}\,\lambda}{2\,v_{Ax}}, \tag{1}$$

where v_{Ax} is the platform velocity, which moves in positive azimuth direction, denoted by x, and λ is the carrier wavelength. The different look angles also imply that the images show the ground at different times. The look bandwidth has to be chosen carefully. If it is too small, the azimuth resolution will decrease, on the contrary if it is too large, the quickly moving objects will be defocused and will lose the point–like property.

The images of the sequence are ground range corrected and then a range migration correction is performed by shifting the images in range direction according to the change of the distance between antenna and ground at different look angles. After this manipulation the stationary background in the images remains at the same position, whereas the positions of the moving objects change from image to image. Due to the single–look processing the images contain a lot of speckle noise. This might be interpreted as a moving object in some cases. To avoid this, a three step algorithm is performed, which evaluates the images of the sequence consecutively, beginning at the image with the highest look center frequency.

3.0 DETECTION AND VELOCITY ESTIMATION OF MOVING OBJECTS

The detection and velocity estimation algorithm consists of three main steps. In the first step candidates for moving objects are detected and in the second step a velocity estimation is performed for each candidate. Finally the candidates are verified to be moving objects.

3.1 DETECTION OF CANDIDATES FOR MOVING OBJECTS

In each image of the generated sequence point–like objects are selected as candidates for moving objects. One candidate consists of several adjoining pixels which have to fulfill the following conditions: The mean intensity of the pixels has to be higher than the mean intensity of the surrounding and the number of pixels has to be between a lower and an upper bound. More details of this algorithm are described in (Kirscht, 1996).

Simultaneously with the detection one gets the shape of the candidates which is later used for compensation of the object velocity.

3.2 VELOCITY ESTIMATION

After having detected candidates for moving objects, for each candidate a displacement vector is estimated using a block matching algorithm as known from e. g. videotelephony (Bierling, 1988). This algorithm estimates the displacement of parts of the image between two successive images s_1 and s_2 of the sequence, which are called frames in this chapter. To obtain the displacement vector, a window is positioned in the frame s_2, so that the candidate lies in the center of it. Then in frame s_1 another window is put at the same position. The aim is, to find the best match between the two windows by shifting the window in frame s_1 on every position within a neighborhood (full search method). For that, one of the following four matching criteria is used, the cross correlation coefficient (CCC), the normalized cross correlation function (NCCF), the mean square error (MSE), and the mean absolute difference (MAD). The NCCF criterion shows the best results. The results of the MSE criterion are nearly as good as the results of the NCCF, with the advantage of a faster implementation. The NCCF is defined by

$$C_{Ns_2s_1}(\Delta x, \Delta y) = \frac{\sum\limits_{x,\,y}\left[s_2(x,y)\cdot s_1(x-\Delta x, y-\Delta y)\right]}{\sqrt{\sum\limits_{x,\,y} s_2^2(x,y)\cdot \sum\limits_{x,\,y} s_1^2(x-\Delta x, y-\Delta y)}}, \tag{2}$$

where (x, y) is one of the positions inside the window, and Δx and Δy are the position shifts between the two windows. Equation (2) has to be evaluated for each different position of the window in the first frame. The motion vector in pixel / frame for the selected candidate is then given by that shifts Δx and Δy which maximize the $C_{Ns_2s_1}$.

The azimuth velocity component is calculated from the displacement vector component $v_{Tx_{pix}} = \Delta x$ in azimuth direction and the range dependent time difference between two successive frames which is given by

$$\Delta t \approx \frac{\Delta\theta\ R_0}{v_{Ax}} \approx -\frac{\Delta f_l\ \lambda\ R_0}{2 v_{Ax}^2} \quad \text{for } \sin\theta \ll 1, \tag{3}$$

where $\Delta\theta$ is the difference between the look angles of adjacent frames, R_0 is the minimal distance between antenna and candidate, and Δf_l is the difference between the look center frequencies.

Let δx be the pixel spacing in azimuth direction, then we can calculate the observed velocity in azimuth direction

$$v_{Tx_{obs}} = \frac{v_{Tx_{pix}}\,\delta x}{\Delta t}\,. \tag{4}$$

This velocity is not the real one, because the objects do not appear at the right positions in the different images. Ouchi showed that the azimuth velocity component has to be divided by a factor of 2 to get the real velocity (Ouchi, 1985) which leads to

$$\hat{v}_{Tx} \approx \frac{v_{Tx_{pix}}\,\delta x}{2\;\Delta t} = -\frac{v_{Tx_{pix}}\,\delta x\;v_{Ax}^2}{\Delta f_l\;\lambda\;R_0}\,. \tag{5}$$

However, this relationship is only exact if the assumption $v_{Tx}/v_{Ax} \ll 1$ is fulfilled.

Here, a more accurate evaluation is made which can also be used with slow platform velocities or quickly moving objects. Let $m_{v_{Tx}}$ be the quotient between observed velocity component $v_{Tx_{obs}}$ and the real velocity component in azimuth direction v_{Tx}, given by

$$m_{v_{Tx}} = \frac{v_{Tx_{obs}}}{v_{Tx}} = \frac{p_{Tx}(t)}{v_{Tx}\;t} \tag{6}$$

where $p_{Tx}(t)$ are the azimuth positions of the moving object at time t. Without loss of generality the azimuth position of the object at time t=0 can be set to $p_{Tx}(t=0) = 0$ because the behavior of the moving objects is nearly independent of the azimuth position. Then in (3) the terms Δt and Δf_l can be replaced by t and f_D, respectively, where f_D is the resulting Doppler shift. With the azimuth positions of the antenna $p_{Ax}(t) = v_{Ax}\;t$ and equation (1), $m_{v_{Tx}}$ becomes

$$m_{v_{Tx}} \approx -\frac{1}{v_{Tx}} \cdot \frac{p_{Ax}(t) + R_0\,\tan\left(\arcsin\frac{f_D\,\lambda}{2\,v_{Ax}}\right)}{\frac{f_D\,\lambda\,R_0}{2\,v_{Ax}^2}}\,. \tag{7}$$

With the approximation $\sin\theta \approx \theta \approx \tan\theta$ and the relation

$$f_D = \frac{2\;(v_{Ax} - v_{Tx})}{\lambda} \cdot \sin\theta \tag{8}$$

one gets

$$m_{v_{Tx}} \approx -\frac{v_{Ax}}{v_{Tx}} \cdot \left(1 - \frac{v_{Ax}^2}{(v_{Ax} - v_{Tx})^2}\right). \tag{9}$$

Finally an azimuth velocity component estimate can be derived using equations (3), (4), (6) and (9) as

$$\hat{v}_{Tx} = v_{Ax} - \sqrt{\frac{v_{Ax}^3}{v_{Tx_{obs}} + v_{Ax}}} = v_{Ax} \cdot \left[1 - \frac{1}{\sqrt{1 - \frac{2\,v_{Tx_{pix}}\,\delta x\,v_{Ax}}{\Delta f_l\;\lambda\;R_0}}}\right] \quad \text{for } v_{Tx_{obs}} > -v_{Ax}. \tag{10}$$

The left hand side of this equation is plotted in figure 1 for a platform velocity of v_{Ax} = 82.5 m/s = 297 km/h. It can be seen that for small velocities v_{Tx} this relation corresponds to the factor 2 which Ouchi calculated.

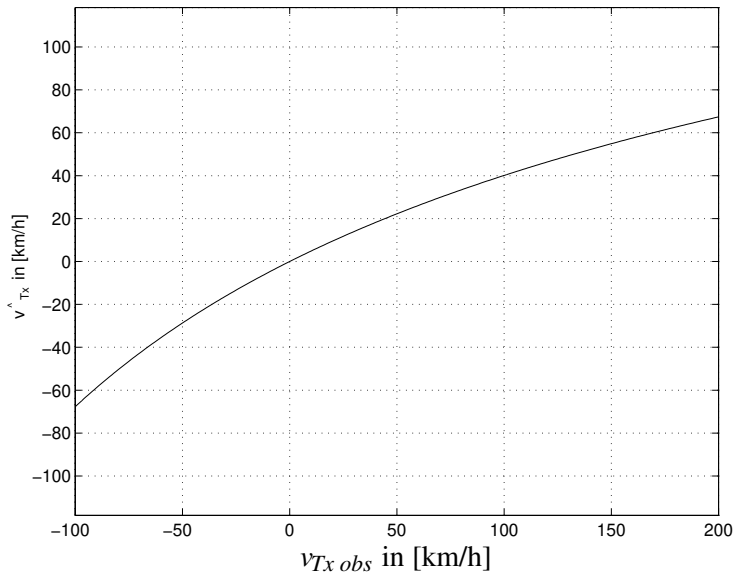

Figure 1. Estimation of the azimuth velocity component v_{Tx} from the observed velocity component $v_{Tx\,obs}$

Until now, mainly the azimuth velocity component of a moving object has been discussed. The observed range velocity component $v_{Ty_{obs}}$ which is obtained from the displacement vector component Δy is not an accurate estimation for the real velocity in this direction. This is because the range positions of objects with a non–zero range velocity component are not correct due to range migration correction. On the other hand, range migration correction is necessary to get a static background. One possibility to avoid this undesired behavior is to compensate the Doppler shift due to motion in range direction prior to the generation of the sequence.

3.3 VERIFICATION OF MOVING OBJECTS

The candidates are verified to be moving objects if their displacement vectors remain quite constant during a fixed number of images. This means that the absolute value and the angle of motion may only change within a fixed range. If this is fulfilled, the counter for this candidate will be incremented and it will be finally detected as moving object, if the dedicated number of images is reached.

Finally, in order to improve the reliability of the estimated azimuth velocity component and the object position, an averaging over all previously counted, estimated values is carried out.

4.0 FOCUSED IMAGING OF MOVING OBJECTS

In order to get a focused image of moving objects on the background, a compensation of the imaging errors is required. Therefore in each single–look image the moving objects are shifted to a reference position using the shape which is known from chapter 3.1. The reference position is attained when the object is broadside the airplane. Approximately this is the averaged position from chapter 3.3 because the observation

interval for each object corresponds with the visibility and detectability in the single–look images of the sequence. Finally, superimposing of the compensated single–look images yields a high quality multilook image with focused moving objects.

5.0 RESULTS

The proposed algorithm has been applied to simulated raw data and to real raw data. A PRF of 1.5 times the clutter bandwidth and a sequence with 16 images are used. The azimuth velocity component v_{Tx} can be estimated with a relative error of 10.9 % for v_{Tx} ranging from –100 km/h (–27.8 m/s) to +50 km/h (+13.9 m/s) and v_{Ty} between ± 30 km/h. For this results the NCCF criterion and simulated raw data of moving objects superimposed on real clutter data are used. All moving objects with a minimum azimuth velocity component of 10 km/h are detected even if they move in direct neighborhood to a strong stationary scatterer. At smaller velocities the detection probability decreases slightly. The maximal detectable velocity can be adjusted; it depends on the maximal Δx in (2) and the maximal number of pixels for the detection of candidates.

In an example two images from a sequence with 16 images are shown. The azimuth direction x runs horizontal. The 5 moving objects in the scene have the velocity components v_{Tx}=30 km/h and v_{Ty} ranging from –20 to +20 km/h. Figure 2 shows image No. 6 of the sequence, where 2 objects out of 5 are already detected, which is marked with a white square. In Figure 3 image No. 11 of the sequence is shown, where all moving objects are detected.

Figures 4 and 5 again show the images No. 6 and 11 of the sequence but now the motion of the objects in azimuth direction is compensated. It can be seen that the objects appear at the same position in

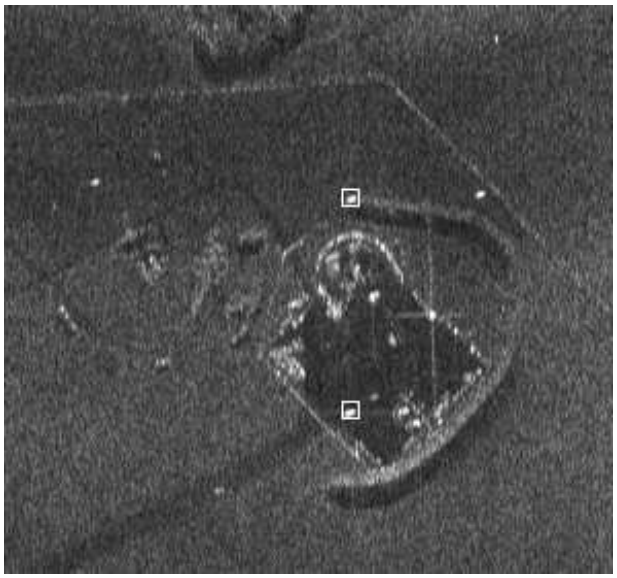

Figure 2. Single–look image No. 6 from the generated sequence, look center frequency is 125 Hz;
2 out of 5 moving objects are detected (marked with a white square)

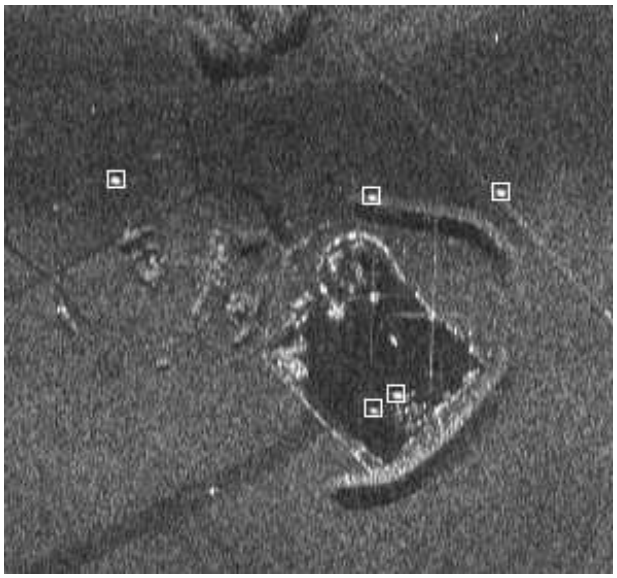

Figure 3. Single–look image No. 11 from the generated sequence, look center frequency is –125 Hz;
all moving objects are detected

both images. The original, wrong positions of the objects appear black. In order to generate a compensated high quality multilook image, multiple compensated single–look images have to be superimposed as shown in Figure 6. In this image the black points are no longer visible and the moving objects appear focused.

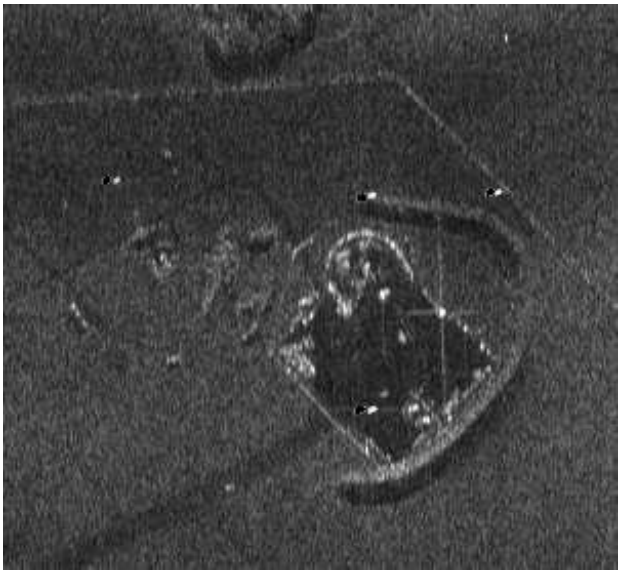

Figure 4. Motion compensated single–look image No. 6 from the generated sequence; the moving objects are shifted to the reference position

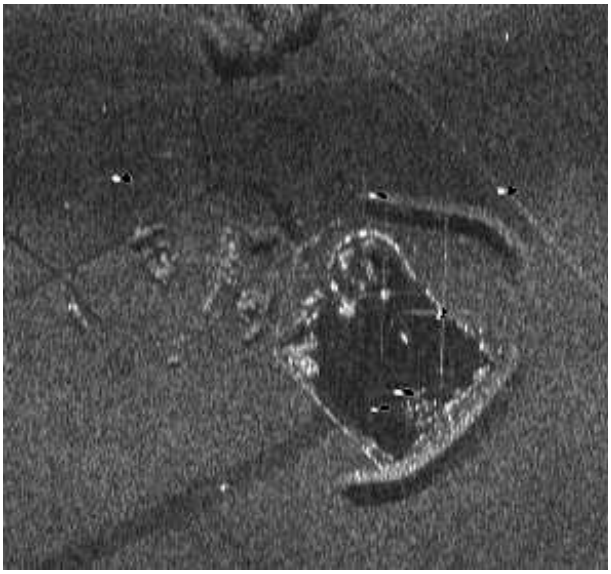

Figure 5. Motion compensated single–look image No. 11 from the generated sequence; the moving objects are shifted to the reference position

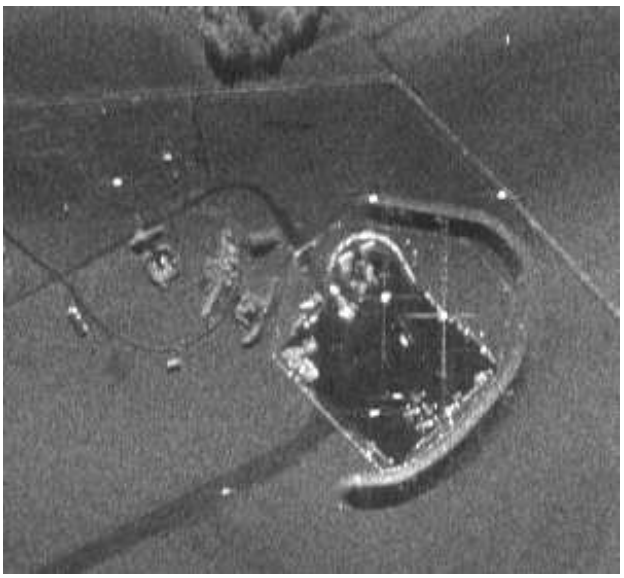

Figure 6. Motion compensated multilook image (8 looks); the moving objects appear focused at the reference position

Applying the method to real SAR raw data also shows good results. Indeed, the detection probability slightly decreases due to the dependence of the reflectivity on the look angle. Experiments show that vehicles like trucks can be detected with high probability.

6.0 CONCLUSIONS

In this paper a method for detection of moving objects and for estimation of their azimuth velocity components has been presented. The method evaluates the temporal correlation in a sequence of single–look SAR images. These images show the ground at different look angles and therefore at different times. By tracking the objects from image to image, the object velocities can be estimated with an absolute relative error of less than 11 %. Using the estimated azimuth velocity component, it is possible to generate multilook images where the defocusing of the moving objects is compensated.

The advantages of the method are, that it works with a small PRF and that also objects can be detected, whose range velocity component is zero. In the future, the current algorithm has to be extended in order to estimate and compensate also the range velocity component.

7.0 ACKNOWLEDGMENTS

This work was supported by the German Federal Government. The author thanks DASA Dornier, Friedrichshafen, Germany, for providing the SAR raw data.

8.0 REFERENCES

- E. D'Addio, M. Di Bisceglie, and S. Bottalico, "Detection of moving objects with airborne SAR." *Signal Processing*, vol. 36, No. 2, pp. 149–162, March 1994.
- S. Barbarossa and A. Farina, "Space–time–frequency processing of synthetic aperture radar signals." *IEEE Trans. Aerospace and Electronic Systems*, vol. 30, No. 2, pp. 341–357, April 1994.
- M. Bierling, "Displacement estimation by hierarchical blockmatching." In *Proc. 3rd SPIE Symposium on Visual Communications and Image Processing*, Cambridge, USA, pp. 942–951, 1988.
- H. Chen and C. McGillem, "Target motion compensation by spectrum shifting in SAR." *IEEE Trans. Aerospace and Electronic Systems*, vol. 28, No. 3, pp. 895–901, July 1992.
- A. Freeman and A. Currie, "Synthetic aperture radar (SAR) images of moving targets." *GEC Journal of Research*, vol. 5, No. 2, pp. 106–115, 1987.
- M. Kirscht, "Detection and velocity estimation of moving objects in a sequence of single–look SAR images." In *Proc. of the International Geoscience and Remote Sensing Symposium IGARSS '96*, Lincoln, Nebraska, USA, pp. 333–335, May 1996.
- K. Ouchi, "On the multilook images of moving targets by synthetic aperture radars." *IEEE Trans. Antennas and Propagation,* vol. AP–33, No.8, pp. 823–827, 1985.
- R. K. Raney, "Synthetic aperture imaging radar and moving targets." *IEEE Trans. Aerospace and Electronic Systems*, vol. AES–7, No. 3, pp. 499–505, May 1971.